Langmuir
Article
pubs.acs.org/Langmuir

A Systematic and Quantitative Study of the Link between Foam Slipping and Interfacial Viscoelasticity

Janine Emile,* Anniina Salonen, Benjamin Dollet, and Arnaud Saint-Jalmes

Institut de Physique de Rennes, CNRS UMR 6521, Université de Rennes I, Rennes, France

Received June 8, 2009. Revised Manuscript Received July 17, 2009

Aqueous foams are often used under various flow regimes, and one of the biggest challenges is to create predictive models of their complex rheological properties. Previous theoretical and experimental studies have qualitatively characterized the wall slip of foams. We focus on this phenomenon in a 1D geometry, studying the friction force to move a train of foam films in a narrow channel. We perform, and correlate, 1D experiments and interfacial measurements of surface elasticity. We adapt existing models to correctly analyze and interpret 1D data, allowing for comparison with 3D foam slip results. Different mixtures of surfactants allow us to quantify the influence of interfacial properties. In particular, we show for 1D experiments that already with a low elasticity, of order 1 mN m^{-1}, we leave the regime where the interface can be considered as fluid, to enter a regime where dissipation depends only marginally on surface elasticity.

1. Introduction

An aqueous foam is a dispersion of gas into a liquid solution, the bubbles being stabilized by surfactants. An important foam parameter is the liquid volume fraction ε, defined as the ratio between the volume of the liquid phase and the volume of the foam. Bubbles for "dry" foams ($\varepsilon < 0.05$) form polyhedral structures with thin separating films and a network of liquid channels, called the Plateau borders. When ε is higher, bubbles are more spherical and less packed. Foams find applications in many industrial areas such as food formulation, detergence, cosmetics, firefighting, etc. Although foams are unstable due to drainage, bubble coarsening, and collapse[1−3] and are inevitably destined to disappear, their lifetime can be considerably increased by optimizing the chemistry in the continuous phase and at the gas−liquid interfaces. In many industrial processes, one of the stakes is to control the properties and stability of a foam under flow conditions, for instance inside a pipe. There is still no general prediction of rheological properties such as yielding, shear thinning, slip at walls, flow uniformity, role of the physical chemistry of the interfaces, and dependence with the liquid fraction and bubble size.[1,4]

One of the problems identified in the foam behavior through channels is related to foam−wall friction and possible slip at surfaces. Different geometries have been used to study the flow properties on macroscopic samples.[5−8] Some results[5] predict that different slip regimes can be obtained depending on the interfacial mobility of the surfactants adsorbed at the interfaces and on the liquid volume fraction. Different laws for the force−velocity relationship are defined, with the power 2/3 in the case of tangentially mobile gas/liquid interfaces (zero interfacial viscoelasticity) or the power 1/2 for tangentially immobile ones. In the first case, the viscous dissipation mainly occurs inside the surface Plateau borders (in contact with the wall), and in the second case, the dissipation occurs mostly inside the wetting film (spread on the solid wall). The differences in the shape of Plateau borders and wetting films are responsible for the different macroscopic behavior.

In order to work on a simplified geometry, another possible setup is proposed: 1D foams constituted by a train of bubbles inside a tube.[9−13] The latter consists of bubbles, stacked one after the other and flowing inside a narrow tube; it can also be seen as separated thin films pushed inside the tube, connected by a liquid film wetting the tube surfaces. A peripheral Plateau border connects the vertical films separating the bubbles from the tube surface and from the continuous wetting film at this surface. This setup has been already used for studies of bubble slipping, in order to determine the relationship between their velocity and the viscous friction. As usual, the experimental and theoretical results are conveniently scaled with the capillary number Ca, defined by $\mu V/\sigma$ where μ is the dynamic viscosity of the fluid, V the relative velocity of the bubble to the solid surface, and σ the gas−liquid surface tension. But the physicochemical properties of the foaming solutions were not controlled: only commercial dish-washing liquids were used.[11,12,14] Particularly, the velocity-dependent thickness of the vertical film separating two bubbles[14] was quantitatively described by a power law, without controlling the system parameters (bubble size, liquid fraction, chemical components). Despite many discussions on the surface rheology, it is not yet established how the slip prefactor, defined in the power law of the friction force, depends on the interfacial viscoelastic properties of the foaming solutions. Only studies realized on the

*Corresponding author: Tel +33 2 23 23 56 46; Fax +33 2 23 23 67 17; e-mail janine.emile@univ-rennes1.fr.

(1) Prud'homme, R.; Kahn, S. *Foams*; Marcel Dekker: New York, 1996.
(2) Exerowa, D.; Kruglyakov, P. *Foam and Foam Films*; Elsevier Science: New York, 1998.
(3) Weaire, D.; Hutzler, S. *The Physics of Foams*; Oxford University Press: New York, 2001.
(4) Liu, A. J., Nagel, S. R., Eds. *Jamming and Rheology: Constrained Dynamics on Microscopic and Macroscopic Scales*; Taylor and Francis: New York, 2001.
(5) Denkov, N. D.; Subramanian, V.; Gurovich, D.; Lips, A. *Colloids Surf., A* **2005**, *263*, 129.
(6) Denkov, N. D.; Tcholakova, S.; Golemanov, K.; Subramanian, V.; Lips, A. *Colloids Surf., A* **2006**, *282*, 329.
(7) Marze, S.; Langevin, D.; Saint-Jalmes, A. *J. Rheol.* **2008**, *52*, 1091.
(8) Raufaste, C.; Foulon, A.; Dollet, B. *Phys. Fluids* **2009**, *21*, 053102.
(9) Bretherton, F. P. *J. Fluid Mech.* **1961**, *10*, 161.
(10) Schwartz, L. W.; Princen, H. M.; Kiss, A. D. *J. Fluid Mech.* **1986**, *172*, 259.
(11) Cantat, I.; Kern, N.; Delannay, R. *Europhys. Lett.* **2004**, *65*, 726.
(12) Terriac, E.; Etrillard, J.; Cantat, I. *Europhys. Lett.* **2006**, *74*, 909.
(13) Saugey, A.; Drenckhan, W.; Weaire, D. *Phys. Fluids* **2006**, *18*, 053101.
(14) Emile, J.; Hardy, E.; Saint-Jalmes, A.; Terriac, E.; Delannay, R. A. *Colloids Surf., A* **2007**, *304*, 72.

steady flows of 3D foams by varying liquid fraction[5] and by using different surfactants to change interfacial properties[5−7,15,16] have given rise to the two foam−wall friction regimes with the scaling laws $Ca^{2/3}$ and $Ca^{1/2}$. If there is a qualitative agreement on the exponents, there is less consensus on the quantitative issues, as different values of the prefactor are found in the literature.[5−13]

In this context, we have extended our work with the 1D setup[12] to perform a systematic and quantitative study with solutions of controlled and characterized properties. Our objectives are the following: to understand how the slip prefactor (in each regime) depends on the interfacial properties and on which interfacial properties (dilatational or shear); to find the balance between physical parameters (liquid fraction, bubble and tube size) and chemical ones. We have also coupled our studies with the interfacial properties: dynamic surface tension and dilatational viscoelasticity. Some rheometry investigations have also been made on 3D foams to compare the results obtained by the 1D setup in order to check whether the 1D and 3D techniques are consistent. More generally, such studies are important for micro- and millifluidics systems with a train of bubbles in capillaries. They present some links to the hydrodynamics problems with free surfaces, meniscus, and surfactants implying coupling between bulk and interfacial viscoelasticity (Bretherton problem,[9] Landau−Levich problem[17]). Indeed, there should exist some general features valid for all these theoretical approaches. Thus, understanding one of them helps to understand the whole family of problems.

In this article, we first describe the setup and the chemicals used, then the results for 1D and 3D foams, followed by the characterization of the interfaces. The 1D data are then analyzed with a model adapted from the one of Denkov et al.,[5] taking into account the specificity of the 1D setup. We finally discuss the relevance and limits of these results and see how foam and interfacial results are correlated and how they can help to solve some of the issues raised in the introduction.

2. Experimental Section

The experiments are carried out with different mixtures of an anionic surfactant, sodium lauryldioxyethylene sulfate (SLES), a zwitterionic surfactant, co-coamidopropylbetaine (CAPB), and myristic acid (MAc). SLES is widely used in shampoos and detergent products, providing good foamability and low bulk viscosity. To improve the foaming stability, cosurfactants like CAPB are commonly added. The role of each component in the foaming solution has been discussed previously[16] and will also be described later in the paper.

All the chemicals were used as received, without additional purification. The foaming solutions are prepared following the protocol of publication.[16] First, 6.6 wt % SLES and 3.4 wt % CAPB are mixed in Millipore water. Then 0.05 or 0.2 wt % MAc is dissolved in the concentrated surfactant solution and heated at 60 °C. Finally, once all the chemicals are dissolved, the solutions are diluted 20 times. The prepared solutions had good stability, without any changes over a month. The bulk viscosity μ was measured to be equal for all solutions: $\mu = 9 \times 10^{-4}$ Pa·s. All experiments are performed at 21 ± 2 °C.

For the 1D foam measurements, we have used a circular glass tube (length $l = 30$ cm and radius $R = 2$ mm). The experiments are performed as in ref 12. The films are prepared by blowing air from an injector immersed in the foaming solution directly in the tube. The liquid fraction, the flow rate, and the position of the nozzle relative to the interface are important parameters to control the foam topology. To obtain the train of bubbles (also known as a "bamboo foam", with equally spaced transverse films), the end of the injector is positioned just at the gas/liquid interface. Once the foam is obtained, gentle rotations are made to evacuate the excess liquid. The average distance L between two consecutive films is constant for a given experiment and varies from 1.54 to 2.54 mm between different runs (see Figure 1). The total mass of solution m_l in the tube is obtained by weighing and all the solution is assumed to be in the Plateau borders, although a part can wet the walls of the tube. This can lead to a slight overvaluation of the liquid volume fraction, ε varies from 0.028 to 0.140, and the value calculated from the ratio v_l/v_f, where $v_l = m_l/\rho$, v_l and v_f are the experimentally measured liquid volume and the estimated foam volume, respectively. The solution density ρ is about 1000 kg m^{-3}. v_f is defined by the relation $v_f = (n-1)L\pi R^2$, where n is the film number, comprised between 15 and 60. The maximum number of films is imposed by the tube length. As soon as the foam is prepared, the films are pushed in the tube with a syringe pump (BS-8000, BIOSEB) at a constant air flow in the range 8−70 mL min^{-1} and at a constant velocity V in the range 3×10^{-3}−30×10^{-3} m s^{-1}. To define the Ca number, we use the value of the surface tension σ when it is stable. We have waited for a long time after the foam production to perform foam experiments in order to stabilize the interface. The surface tension values of the different foaming solutions are given in the next section. One tube end is at the atmospheric pressure, whereas the pressure at the other end is recorded by a pressure transmitter (Kellor, series 41, range 10 mbar). Several forward and backward shifts of the foam within the tube are made to measure the pressure, giving a dispersion of the order of 5%. To avoid any evaporation problem, the length of every measurement, pressure versus the velocity for a given liquid volume fraction, is about 30 min.

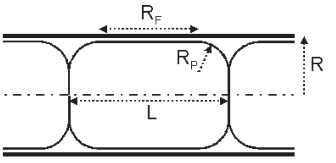

Figure 1. Sketch of the train of foam films, with the main geometrical parameters.

The 3D foams are produced using a turbulent mixer apparatus.[18] Experiments were performed with a Physica MCR 301 rheometer (Anton Paar), equipped with a plate−plate geometry (diameter = 74.905 mm and gap = 3 mm). A smooth surface is used on the bottom plate to provide wall slip. The top plate is rotated at controlled velocity, varied from 7.64×10^{-3} to 7.64 rpm, and the slip stress, τ_w, is measured. More details on the experimental protocol and the data interpretation procedure are described in refs 5 and 7.

The interfacial tension and the surface dilatational properties of the foaming solutions are measured using an oscillatory rising bubble tensiometer (Tracker Teclis-IT Concept, France).[19] From the shape of a bubble, attached at the tip of a syringe, one can deduce the surface tension σ as a function of time (starting at 1 s after the formation of a "naked" bubble inside the solution). The estimated error of measured values of the surface tension is ~0.2 mN m^{-1}. The viscoelastic properties were determined by the same setup, with bubble area sinusoidal oscillations of relative amplitude $\delta S/S_0$. Oscillations are performed 30 min after drop formation, once the interfaces are in equilibrium. The frequency dependencies of the dilatational moduli are determined by varying the oscillation frequency from 0.025 to 0.25 Hz. For the given frequency 0.2 Hz, $\delta S/S_0$ is defined in the range 0.65−20.80%. An

(15) Tcholakova, S.; Denkov, N. D.; Golemanov, K.; Ananthapadmanabhan, K. P.; lips, A. *Phys. Rev. E* **2008**, *78*, 1.
(16) Golemanov, K.; Denkov, N. D.; Tcholakova, S.; Vethamuthu, M.; Lips, A. *Langmuir* **2008**, *24*, 9956.
(17) Landau, L. D.; Levich, V. G. *Acta Physicochim. URSS* **1942**, *17*, 42.
(18) Saint-Jalmes, A.; Vera, M. U.; Durian, D. J. *Eur. Phys. J. B* **1999**, *12*, 67.
(19) Benjamins, J.; Cagna, A.; Lucassen-Reynders, E. H. *Colloids Surf.* **1996**, *114*, 245.

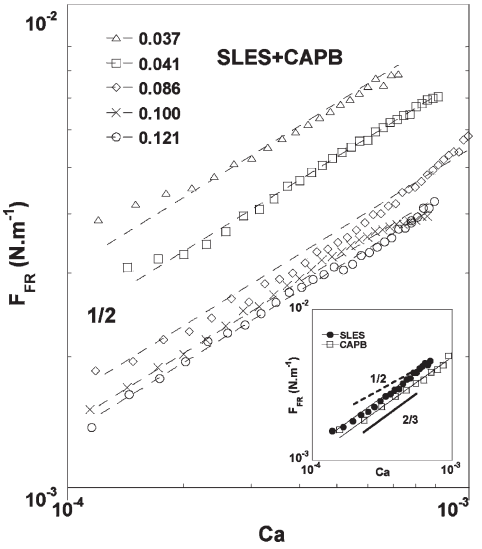

Figure 2. 1D foam data of SLES + CAPB. Friction force per unit length as a function of the capillary number $Ca = \mu V/\sigma$, for different liquid volume fractions. The data are fitted by a power law with an exponent 1/2. Inset: data for each surfactant, SLES ($\varepsilon = 0.13$) and CAPB ($\varepsilon = 0.10$).

example of bubble surface area and surface tension oscillations obtained by this technique was presented in ref 20.

The surface dilatational modulus, E_D, is analyzed using the Fourier transformation (FT): $E_D = \mathrm{FT}[\delta\sigma]/\mathrm{FT}[\delta S/S_0]$, where σ is the surface tension. According to its definition, E_D completely characterizes the dilatational behavior of a given interface. E_D is a complex quantity, with real and imaginary components, $E_D = E_{DS} + iE_{DL}$. E_{DS} is the surface elastic "storage" modulus, which measures the energy stored during an interfacial deformation. E_{DL} is the loss modulus related to surface dilatational viscosity, accounting for energy dissipation through different relaxation processes, such as diffusion of surface-active species from the bulk as well as interfacial reorganization of adsorbed species.

3. Results and Interpretation

1D Foam Data. We have measured the velocity of the film train moving along the tube under an applied driving pressure ΔP. To facilitate comparison of our measurements to a model, we will report, instead of ΔP, the friction force per spanwise length of a bubble F_{FR}, introduced by Denkov et al.[5,6] To do so, we first apply a force balance on the train of n films: $\pi R^2 \Delta P = nF_B$, with F_B the friction force per bubble, related to F_{FR} through the tube perimeter: $F_B = 2\pi R F_{FR}$; therefore, $F_{FR} = R\Delta P/2n$. We assume for simplicity that we can ignore end effects, which is reasonable given the high number of films ($n \geq 15$).

Figure 2 represents the friction force of the SLES + CAPB foams, for different liquid volume fractions ε, versus the capillary number Ca. The force increases when ε decreases with a well-defined $Ca^{1/2}$ dependence for $2 \times 10^{-4} \leq Ca \leq 10^{-3}$. For each surfactant, individually, the power law for the foam−wall friction is proportional to $Ca^{2/3}$, as expected for "mobile" surfaces (inset of Figure 2). As soon as mixtures are considered, the power law is given by $Ca^{1/2}$; the slip exponent 1/2 is associated with "rigid" surfaces. Our recent investigations indicate that this 1/2 exponent is found regardless of the number of films, including a single film.

(20) Loglio, G.; Pandolfini, P.; Miller, R.; Makievski, A. V.; Ravera, F.; Ferrari, M.; Liggieri, L. Drop and bubble shape analysis as tool for dilational rheology studies of interfacial layers. In *Novel Methods To Study Interfacial Layers*; Möbius, D., Miller, R., Eds.; Elsevier: Amsterdam, 2001; pp 439−484.

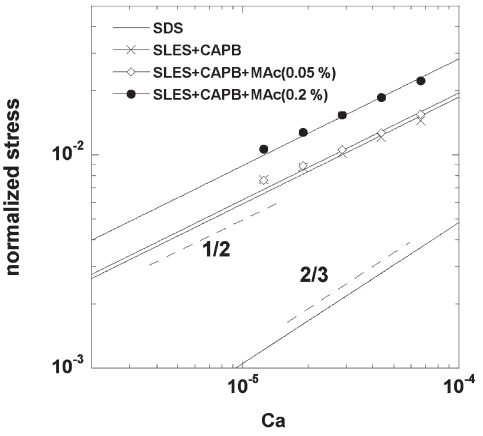

Figure 3. Viscous stress normalized by Laplace pressure, σ/R_B (R_B is the bubble radius) versus the capillary number for foams of different surfactant solutions. The dotted lines are drawn as guides to the eye with the slope indexes 1/2 and 2/3.

Similarly and before further analysis, we report the raw data obtained for the 3D foams. Figure 3 shows the dependence of normalized stress (slip stress τ_w divided by Laplace pressure, σ/R_B, where R_B is the bubble radius) on the capillary number Ca, following the usual convention found in previous works.[5,7] The liquid fraction is constant and equal to 0.15. Results for SLES + CAPB with and without MAc are plotted, together with an older result[7] for pure sodium dodecyl sulfate, SDS (similar to pure SLES), for comparison.

As for the 1D geometry, a single value of the slip exponent equal to 1/2 is found for the SLES + CAPB and SLES + CAPB + MAc. In all these cases, there is clearly much more dissipation in these mixed systems than for a single surfactant solution; the SDS foam curve is well below the other ones and shows a slip exponent close to 2/3. Note also that there is almost no difference between the SLES + CAPB and SLES + CAPB + MAc (0.05%). Only with the largest amount of MAc (0.2%), a small increase of the stress is observed. Between no myristic acid and 0.2% of MAc, the ratio of the prefactor of the power law is equal to $2.80/1.95 \approx 1.4$.

Back to the 1D geometry, Figure 4a represents the dimensionless slip prefactor, $F_{FR}/\sigma Ca^{1/2}$, versus the liquid volume fraction ε, for different amounts of MAc. From the figure, one can observe two specific features. First, the dimensionless slip prefactor, within the error bars, is the same for SLES + CAPB and SLES + CAPB + MAc (0.05%). However, the difference is slightly visible for SLES + CAPB + MAc (0.2%). Second, the value of the prefactor increases strongly for dry foams ($\varepsilon < 0.05$), whatever the composition of the mixture. In the extreme case of a very dry foam, it seems difficult to distinguish between different types of solutions used.

For this 1D geometry, to date no theoretical explanation of the form of the dependence on liquid fraction has been defined. Denkov et al.[6] have developed a model relating F_{FR} to the capillary number and the liquid fraction for a foam; we now adapt their predictions to the geometry of our system. These authors calculated the friction force between a bubble and a wall in the case of rigid interfaces (for which the no-slip boundary condition applies), based on a 2D computation in the streamwise plane perpendicular to the wall. The friction force per bubble writes

$$F_B = \left| \int_{A_B} \mu \left(\frac{\partial V_x}{\partial z} \right)_{z=0} \mathrm{d}A \right| \quad (1)$$

where A_B is the projected bubble area on the wall surface, V_x the streamwise velocity component, and z the axis locally

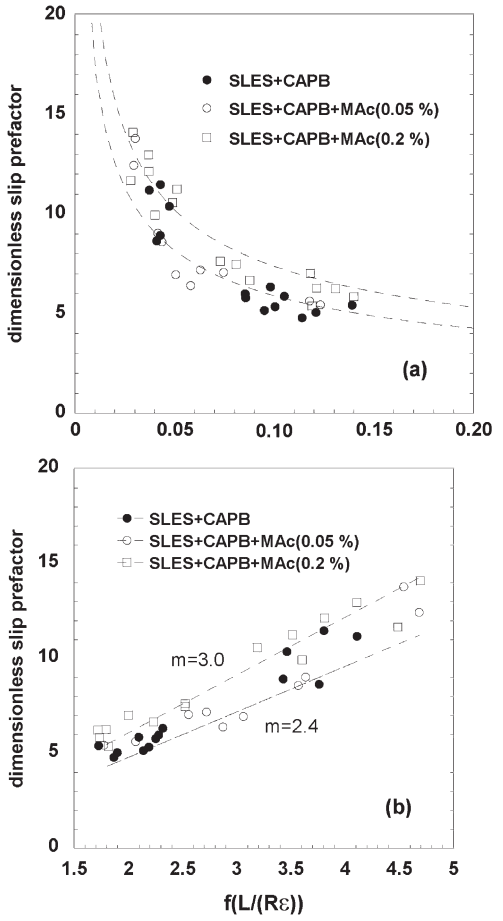

Figure 4. (a) Dimensionless slip prefactor $F_{FR}/\sigma Ca^{1/2}$ as a function of the liquid volume fraction, for 1D foam of SLES + CAPB with or without myristic acid (the dotted lines serve as guides to the eye). (b) Dimensionless slip prefactor as a function of $f(L/(R\varepsilon)) = [((4-\pi)L/(\varepsilon R))^{1/2} - 2]^{1/2}$. The data with SLES + CAPB, SLES + CAPB + MAc (0.05%), and SLES + CAPB + MAc (0.2%) are fitted by a straight line of slope $m = 2.4$ and $m = 3.0$, respectively.

perpendicular to the wall, located at $z = 0$ (see Figure 1 from ref 6). This is strictly equivalent to eq 16 in ref 6, except that we reason directly on the whole bubble and not per unit length in the spanwise direction. Since the thickness of the wetting film, where most of the dissipation occurs remains small compared to the tube radius R, we can use the expression of Denkov et al.[6] for the friction force per unit (spanwise) length of a bubble, given by eq 25 in ref 6:

$$F_{FR} = 2.50\sigma\left(\frac{CaR_F}{R_P}\right)^{1/2} + \sigma\left[7.0Ca^{3/4} - 8.5\left(\frac{R_P}{R_F}\right)^{1/4}Ca\right] \quad (2)$$

where R_P is the Plateau border radius (meniscus region) and R_F the "film radius", which in our geometry equals $R_F = (L - 2R_P)/2$ (Figure 1).

We further neglect in F_{FR} the second term on the right-hand side, i.e., the contribution of the transition regions between the wetting films and the Plateau borders; this is reasonable if $Ca^{1/4}(R_P/R_F)^{1/2} \ll 1$, which is always the case since our highest capillary number is $Ca = 10^{-3}$ and our highest ratio $R_P/L = 0.38$, hence, $Ca^{1/4}(R_P/R_F)^{1/2}$ is always lower than 2×10^{-3}. Hence, we have

$$F_{FR} = 1.77\sigma\left(\frac{Ca(L-2R_P)}{R_P}\right)^{1/2} \quad (3)$$

Note that this expression involves the three characteristic lengths of the system: the tube and Plateau border radii and the separation between two consecutive films, whereas there are only two such lengths in a 3D foam against a wall: the Plateau border and bubble sizes. This means that, contrary to a 3D foam, the friction will not only be a function of the capillary number and the liquid volume fraction; an additional combination of geometrical parameters is required.

We do not have a precise measurement of the Plateau border radius; however, it is much bigger (0.1−1 mm) than the wetting film thickness, about 0.1−1 μm;[6] hence, it is reasonable to assume that all the solution is located in the Plateau borders, which gives us a way of relating R_P to the liquid volume fraction, which is measured precisely by weighing. The comparison between the hydrostatic pressure, $\rho g(2R)$, and the capillary pressure in the Plateau border, $2\sigma/R_P$, shows that drainage remains insignificant (estimated finished within 5 min). Hence, R_P is constant over the tube periphery; therefore, the volume of a single Plateau border writes $V_{PB} = \int_0^R 2\pi(R-z) \times 2e(z)\,dz$, where the lateral dimension $e(z)$ of the Plateau border equals

$$e(z) = R_P - (R_P^2 - (z - R_P)^2)^{1/2} \quad \text{for } 0 < z < R_P \text{ and 0 else} \quad (4)$$

Hence

$$V_{PB} = \pi R_P^2\left[(4-\pi)R - \left(\frac{10}{3} - \pi\right)R_P\right] \quad (5)$$

The liquid is assumed to be contained principally in the Plateau borders. So the liquid volume fraction ε is the ratio between the volume of a Plateau border and the one per film: $\varepsilon = V_{PB}/\pi R^2 L$; assuming that $(4 - \pi)R \gg (10/3 - \pi)R_P$, which is less restrictive than the condition $R \gg R_P$, we have the following relation between R_P and ε: $R_P \approx (\varepsilon RL/(4 - \pi))^{1/2}$; thence, the prediction of the friction force as a function of the capillary number, the liquid volume fraction, and the geometrical parameter L/R:

$$F_{FR} = 1.77\sigma Ca^{1/2}\left(\left(\frac{4-\pi}{\varepsilon}\frac{L}{R}\right)^{1/2} - 2\right)^{1/2} \quad (6)$$

Following this new theoretical prediction, the prefactor defined by $1.77[((4-\pi)L/(\varepsilon R))^{1/2} - 2]^{1/2}$ is thus not a simple law of ε. The distance L between the films and ε are strongly correlated. Figure 4b shows that the slip prefactor is a function of $f(L/R\varepsilon) = [((4 - \pi)L/(\varepsilon R))^{1/2} - 2]^{1/2}$. As expected from the model, the dependence is linear; however, the slope is slightly higher than the predicted factor 1.77. There are some fluctuations of the prefactor values, which seem to result from temperature variations of the bulk viscosity μ. There is a slight dependence on the surfactant solution which becomes more significant with the concentration of MAc added in the foaming solution. The experimental value of the slope m extracted from a linear fit is 2.4 and 3.0 for SLES + CAPB or SLES + CAPB + MAc (0.05%) and SLES + CAPB + MAc (0.2%), respectively. Note that we found here a similar ratio as for the 3D foams: $2.80/1.95 \approx 1.4$ (3D) in comparison with $3.0/2.4 \approx 1.3$ (1D). We will come back to some of these results in the Discussion section in order to see whether these are consistent with the interfacial rheology data presented below.

Interfacial Rheology. Figure 5 illustrates the time dependencies of the surface tension of SLES + CAPB solutions containing MAc. It is seen that with increasing MAc concentration the long-time constant value of the surface tension slightly decreases, but the time taken to reach this value increases. A stable value of the

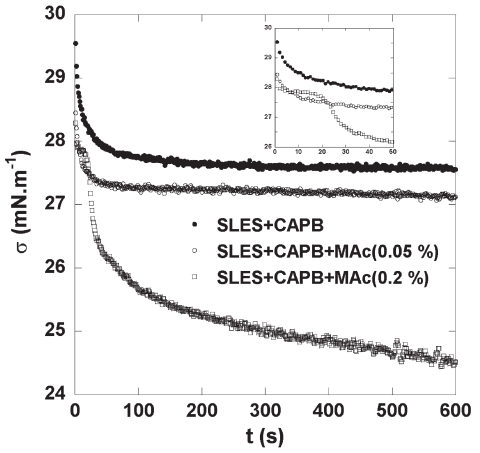

Figure 5. Dynamic surface tension σ of the three different foam solutions used in the study, obtained with the rising bubble tensiometer. Inset: enlargement of the same figure at shorter times.

surface tension is reached at $\sigma = 27.55$ mN m^{-1} after 300 s for SLES + CAPB and $\sigma = 27.11$ mN m^{-1} after 500 s for SLES + CAPB + MAc (0.05%). On longer time scales (up to 5000 s), it is found that the surface tension of SLES + CAPB + MAc (0.05%) has a very slow and progressive decrease (about 1 mN m^{-1}) occurring after about 2000 s (30 min). For a higher MAc concentration (SLES + CAPB + MAc (0.2%)), a plateau region at short times (between 2 and 20 s) is seen, and the equilibrium state, $\sigma = 24.15$ mN m^{-1}, is obtained after 900 s. In order to explain the results, we should remember that SLES and CAPB are needed to solubilize the fatty acids (MAc) and to form mixed micelles in solution.[16] The origin of the plateau may be explained by a micellar diffusion followed by decomposition liberating acid molecules to form the mixed surface layer, which is not instantaneous. We also note that the surface tension values of these foaming solutions are finally very close and that the major part of the adsorption occurs within less than 1 s, as could be expected from the concentration of SLES and CAPB used. The effect of acid is mainly observed in the slow adjustment due to the formation of mixed layers, as predicted by theory.[21]

The total dilatational modulus, E_D, has been measured versus the relative surface deformation at a frequency of 0.2 Hz. Figure 6 shows clearly that SLES + CAPB and SLES + CAPB + MAc (0.05%) solutions have very low surface moduli. Note that we have found similar results for the pure SLES and CAPB solutions. The characteristic exchange frequency between surface and bulk is larger than the frequency of the applied dilatation, and the surface tension response is instantaneous. However, the SLES + CAPB + MAc (0.2%) solution exhibits a rather high surface modulus with the value decreasing rapidly with the surface deformation. At all surface deformations, it is mainly the loss (viscous) surface dilatational modulus E_{DL} which contributes in the values of E_D (the value of the elastic surface dilatational modulus E_{DS} is about 20 mN m^{-1} and remains constant for $\delta S/S_0$ superior to 5%). We have also investigated the variation of the surface modulus with changing oscillation period. For a relative surface deformation $\delta S/S_0$ of 2%, the inset of the Figure 6 represents the results for the 0.2% MAc sample: the overall modulus E_D continuously decreases when the oscillation period increases; nevertheless, even with a slow oscillation of period 40 s, the modulus is still large and of a few tens of mN m^{-1}.

(21) Ariel, G.; Diamant, H.; Andelman, D. *Langmuir* **1999**, *15*, 3574.

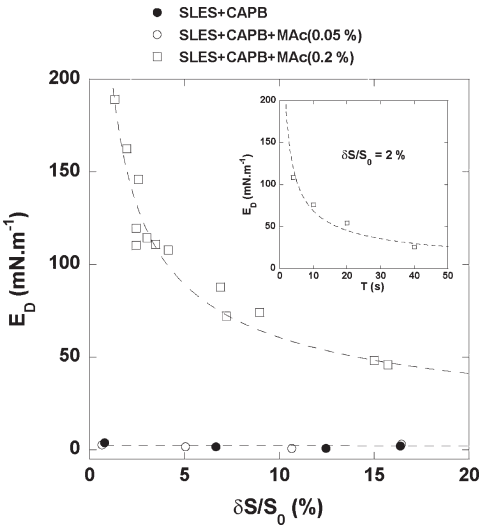

Figure 6. Total surface dilatational modulus, E_D, of foaming solutions, as a function of the relative surface deformation, measured by drop-shape analysis of oscillating pendant drops (5 s oscillation period). Inset: total surface dilatational modulus of SLES + CAPB + MAc (0.2%) solution for a relative surface deformation of 2%, as a function of the oscillation period.

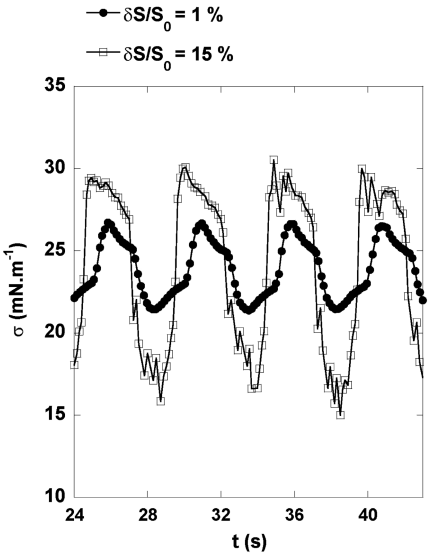

Figure 7. Oscillations of the surface tension for a drop of SLES + CAPB + MAc (0.2%) with period of 5 s with two relative surface deformation values, $\delta S/S_0 \approx 1\%$ and $\delta S/S_0 \approx 15\%$.

The existence of such high values for the compression modulus for 0.2% of MAc, even at high oscillation periods, indicates that the interface behaves more and more like an insoluble layer as the concentration of acid is increased. The low solubility of the MAc molecules, meaning slow desorption, explains how the layer can still resist elastically to compression at high periods. As well, we also want to point out that when imposing a sinusoidal oscillation of the bubble area, the surface tension does not show a nice sinusoidal response (as found for usual surfactants); in fact, as shown in Figure 7, the response has a complex shape (whatever the oscillation amplitude).The SLES + CAPB + MAc interface thus appears like a complex system, with the mixing of highly soluble and insoluble species. The coupling between the dynamics of adsorption/desorption of the different molecules is revealed in the unusual shape of the surface tension in Figure 7 and might also be responsible for the loss modulus being higher than the storage

modulus. In spite of the complex response to the dilatational oscillations, Brewster angle microscopy measurements show that this mixed interfacial layer is actually homogeneous, discarding a potential phase separation within the interface.

4. Discussion

The experiments presented show that qualitatively the 1D foam slip experiments are in agreement with the existing theory regarding the viscoelastic properties of the surfactants used; thus, an exponent of 1/2 is observed with solutions where high dilatational moduli are found and conversely 2/3 in systems with fluid interfaces. By correctly taking into account the specificity of the ID geometry, we have been able to show that 1D and 3D experiments are in agreement. However, surprisingly, the regime change between mobile and immobile surfaces was found to occur at much lower than expected E_D. In the regime where dissipation is dominated by the wetting films, for which $F_{FR} \sim Ca^{1/2}$ (from E_D of a few mN m^{-1}), we have shown that even a drastic modification of the interfacial properties makes only a small quantitative change: the slip prefactor varies by only 30% as E_D changes by 2 orders of magnitude (Figures 4b and 6).

The presence of a corrective term $f(E_D)$ which is related to E_D, is required in the formula for the friction force to accurately describe the response. Following the formalism described in ref[7] for 3D foams, the normalized viscous stress needed for slip as a function of the capillary number, in the regime of $Ca^{1/2}$, is weighted by the prefactor noted C_{FILM}, corresponding to viscous dissipation inside the wetting film. In these conditions, C_{FILM} is analogous to the corrective term $f(E_D)$. A detailed description of $f(E_D)$ or C_{FILM} remains elusive, although we have shown that 1D/3D methods give identical results, and thus combinations of experiments can be used to help further validate theoretical predictions. Unfortunately, presently systems with highly tunable interfacial properties are still missing (experiments with solutions containing 0.1% and 0.4% of MAc give interfacial values very close to that of the solution with 0.2% MAc) and therefore does not allow for quantitative information about the parameters $f(E_D)$ or C_{FILM} to be given. However, the use of the mixed surfactant system, as used in the present study, is a useful step forward. Although the viscoelastic properties of the system are important to fully understand the flow behavior, an even stronger dependence of the slip dissipation is observed depending on the structure of the foam, i.e., liquid fraction ε, bubble size R, and the length of the bubble L.

In order to draw insightful conclusions from the combination of foam experiments and interfacial measurements, the comparability of the two methods should be verified. Indeed, given the strong dependence of the surface modulus on the frequency and relative area deformation measured with the tensiometer for the SLES + CAPB solution with 0.2% MAc, one may wonder whether the tensiometer data are of any relevance for the film train (1D) experiments, all the more because the two setups have very different geometries. We propose to estimate the most relevant kinetic parameter to compare both situations: the rate of interfacial deformation. For the tensiometer, the bubble oscillations generate a pure surface dilatation/compression, with a typical deformation rate of order $\omega\delta S/S_0 \approx 10^{-2}-10^{-1}$ s^{-1}. In the film train, the interface is compressed in front and extended behind the moving film. To estimate the associated deformation rate, we adapt the model of Hirasaki and Lawson,[22] who took into account the presence of surfactants in film trains. The interfacial velocity gradient dV/dx with coordinate x parallel to the tube axis, is as follows:

$$\frac{dV}{dx} = \frac{(3Ca)^{1/3}}{0.643}\frac{V}{R_P}\frac{d\omega}{d\xi} \tag{7}$$

with the dimensionless velocity gradient $d\omega/d\xi$ expressed from the eq 32 of ref 22:

$$\frac{d\omega}{d\xi} = \frac{4}{\sqrt{N_S}}\frac{1-e^{-N_L}}{1+e^{-N_L}} \tag{8}$$

The parameters N_S (eq 27a[22]) and N_L (eq 34a[22]) are deduced from our experimental conditions:

$$N_S = \frac{E_D}{0.643\mu\alpha R_P} \tag{9}$$

and

$$N_L = \frac{2(3Ca)^{-1/3}}{0.643\sqrt{N_S}}\frac{(L-2R_P)}{R_P} \tag{10}$$

For the expression of the parameter N_S, the mass transfer rate constant, α (eq 17[22]) is assumed to be related to the typical time scale of the relaxation of the dynamic surface tension (see Figure 5). With our experimental values $V = 10^{-2}$ m s^{-1}, $\sigma = 25$ mN m^{-1}, $Ca = 4 \times 10^{-4}$, $\mu = 10^{-3}$ Pa s, $R_P = 0.1$ mm, $L = 2$ mm, and $\alpha = 10^{-2}$ s^{-1}, one finds

$$N_S \approx 10^9 E_D \text{ and } N_L \approx \frac{-10^{-2}}{\sqrt{E_D}} \ll 1$$

hence

$$\frac{d\omega}{d\xi} \approx \frac{2N_L}{\sqrt{N_S}} \text{ and } \frac{dV}{dx} \approx \frac{10^{-3}}{E_D}$$

Since we measured $E_D \approx 10^{-1}$ N m^{-1} with the tensiometer, we expect in the film train a typical deformation rate of 10^{-2} s^{-1}, which is indeed the same order of magnitude as that imposed by the tensiometer. Hence, despite the differences in geometry and confinement, the tensiometer and the film train impose comparable deformation rates at the interface, which justifies a posteriori the relevance of comparing the interfacial measurements of the tensiometer to the film train results. In other words, at least the order of magnitude of E_D measured by the tensiometer is applicable to the film train configuration; a quantitative correspondence is more questionable, given the complex dependence of E_D on both the relative surface variation and the frequency displayed in Figure 6.

The validity of comparing the two types of measurements has been shown, however, to further explain the small value of E_D apparently required for the surfaces to be considered as rigid (a few mN m^{-1}); we should consider another interesting feature of the model of Hirasaki and Lawson. These authors predicted (see eq 37b in ref 22) that the pressure drop per film writes

$$\Delta P = \frac{8}{3}\frac{\sigma}{R}(3Ca)^{2/3}\sqrt{N_S}\frac{1-e^{-N_L}}{1+e^{-N_L}}$$
$$\approx \frac{8}{3}\frac{\sigma}{R}(3Ca)^{2/3}\sqrt{N_S}\left[\frac{N_L}{2} + O({N_L}^3)\right] \tag{11}$$

From the definition of N_S and N_L, we can see that ΔP tends toward a constant value, independent of E_D, at small N_L, hence at

(22) Hirasaki, G. J.; Lawson, J. B. *Soc. Pet. Eng. J.* **1985**, *25*, 176.

high surface modulus. However, interestingly, $N_L \approx -10^{-2}/E_D^{1/2}$ is already smaller than one (its value is 0.22) for SLES + CAPB without MAc; hence, SLES + CAPB is already in the "high modulus" limit in the present case and the SLES + CAPB + MAc mixtures even more so. This is coherent with the weak increase of the overall friction even when E_D increases by 2 orders of magnitude, and it could be tempting to adapt Hirasaki and Lawson's model to get a theoretical prediction of the correction factor $f(E_D)$ in eq 7. However, in this "high modulus" limit, this model predicts an exponent 1/3 for the capillary number:

$$\Delta P \approx 5.98 \frac{\sigma}{R} Ca^{1/3} \frac{L - 2R_P}{R_P} \quad (12)$$

which is inconsistent with the experiments. Therefore, there exists no single model able to capture both our experimental dependences on Ca and E_D: the model of Denkov et al.[5,6] is successful in predicting the dependence on Ca, but it is limited to purely rigid interfaces. On the other hand, the model of Hirasaki and Lawson[22] deals with arbitrary surface moduli but does not predict the right exponent on Ca. An accurate theoretical description should probably combine aspects from both models.

Our results are in qualitative agreement with the existing literature, since the friction force follows a power law which differs between mobile and immobile interfaces, as expected. However, some discrepancies are observed on the slip prefactor: the most rigid system in our case had a slope of 3.0, which is slightly higher than the theoretically predicted 1.77.

The transition from fluid to rigid interfaces was observed at very small dilatation moduli, which might be explained following the formalism of Hirasaki and Lawson.[22] This contrasts with previous studies (cf. Table 2 of refs 5 and 16), where surfactants with low surface dilatational moduli always exhibited the power law $Ca^{2/3}$ for the foam−wall friction. Here, for SLES + CAPB solutions, we have clearly measured a power law index of 1/2 although it has a low value of $E_D = 2.0 \pm 1.7$ mN m^{-1}. However, we have also found that the pure surfactant solutions provide a "mobile" response (exponent 2/3), while their interfacial elasticities are also very low. Therefore, there are problems with the classification of the surface properties using a single measurement of surface dilatational viscoelasticity. Moreover, it seems that such measurement should also be very accurate, especially in the range of low values (between 0 and 5 mN m^{-1}), in order to discriminate between systems. On this special case of SLES + CAPB and for the comparison with previous works,[5,16] note that we are not using the same chemical supplier and that the solutions are then not rigorously identical; differences in the composition and purity of the surfactant could lead to small interfacial changes, sufficient to change the dissipation regime. Another example of problem of classification using only the dilational elasticity is the counterintuitive case of potassium cocoylglycinate: a surface modulus E_D of 56 mN m^{-1} was measured but classified as a surfactant providing mobile interfaces because of the $Ca^{2/3}$ law (see Table 2 of ref 5). In this particular case, this could indicate that potassium cocoylglycinate might be an interesting "intermediate system": being able to behave like a rigid or a mobile surfactant depending on the perturbation. Indeed, our preliminary tests with these molecules show that the modulus varies strongly between low and high values within the usual range of frequency and amplitude variations provided by the tensiometer. Further stressing the fact that a single value of E_D is informative but not sufficient to classify a surfactant interface as "mobile" or "immobile" due to the dependence on the type of excitation and that the dependence on other experimental conditions (deformation rate, fluid fraction, bubble size, geometry of the setup) is also crucial.

Furthermore, as we have shown (Figures 6 and 7), the interfacial response of the used surfactant mixtures SLES + CAPB + MAc are extremely complicated. During the dilatation, there is a phase shift between the excitation surface function and the tension response with a decrease in "sawtooth" form. It is probably due to the adsorption time of the surfactants, which differs from that of acids. In any case, the nonlinear response of the surface shows that it cannot be characterized only by a single value of the surface modulus, but rather by its full spectrum. Note also that one should also be aware that the presence of MAc at the interface could lead to phase separation and to domains of condensed phase; moreover, the time required to obtain this specific interfacial texture might be different from one setup to another (long times required at the pendant drop interface and faster time in the films and foams). Such effects can then be responsible for differences in the interfacial properties between our various experimental configurations and adding some complexity. In that respect, the surfactant mixtures containing nonsoluble compounds, like MAc, might not be an ideal model systems to understand the surface dilatational deformations, although the foaming solutions give us encouraging results to continue these studies.

5. Conclusion

New experiments on the flow of a train of foam films in a tube have been performed by controlling the physical chemistry of studied solutions. These investigations have been coupled to interfacial measurements of surface elasticity. Different mixtures of surfactants have allowed us to quantify the influence of interfacial properties. For the 1D geometry of the train of films, the friction force is defined by a function of the capillary number, the liquid volume fraction, the geometrical parameter L/R (ratio between the film distance and the tube radius), and the surface rheology. In the regime where viscous dissipation scales with the capillary number with a power 1/2, we have confirmed that liquid fraction has a much stronger influence on the quantitative value of friction than surface elasticity. To correctly analyze and interpret 1D data, we have adapted existing models, thus allowing for comparison with 3D foam slip results. An estimation of the deformation rate in both setups showed that interfacial measurements and 1D experiments are compatible. We have shown for 1D experiments that the transition between the regime where the interface can be considered as fluid, and the regime where dissipation depends only marginally on surface elasticity, occurs for a small critical surface elasticity, of the order of a few mN m^{-1}, and hardly measurable with accuracy. Because of the complex amplitude and frequency dependence of the surface dilatational properties, a single value of the surface viscoelastic modulus cannot be defined. Thus, further theoretical efforts are needed to elucidate surface rheological mechanisms and their role in foam slip.

Acknowledgment. We are grateful to Sylvie Beaufils and Isabelle Cantat for the useful discussions on surface rheology. The authors thank the Agence Nationale pour la Recherche (ANR-07-BLAN-0340).